*J. Plasma Physics* (2010), *vol.* 76, *parts* 3&4, *pp.* 525–537. © Cambridge University Press 2010 
doi:10.1017/S0022377809990675

# Dusty plasma processes in Earth's environments containing nano- and microscale grains

SERGEY I. POPEL

Institute for Dynamics of Geospheres RAS, Leninsky prospect 38, building 1, 119334 Moscow, Russia
(s_i_popel@mail.ru)

(Received 2 December 2009 and accepted 7 December 2009, first published online 13 January 2010)

**Abstract.** Review of plasma processes in the Earth's environments containing nano- and microscale grains is presented. Possible observational manifestations of dusty ionospheric plasmas during high-speed meteor showers are described. A unified explanation of ionization properties of the polar mesosphere under summer conditions is given. Dusty plasma processes are also considered in application to active geophysical rocket experiments which involve release of some gaseous substance in near-Earth space, the origin of the primary Earth's crust, hydrosphere and atmosphere, and global electromagnetic Schumann resonances.

## 1. Introduction

Processes taking place in plasmas containing charged nano- and microscale particles have been the subject of extensive studies in recent years [1–3]. Systems of this kind are generally called dusty (or complex) plasmas. In nature, charged dust grains are present in planetary magnetospheres and ionospheres, atmospheres of comets, and interstellar medium [4–6]. In the Earth's troposphere, dust from natural and anthropogenic sources is present at different altitudes. The dust can ascend to the stratosphere and ionosphere in the course of violent volcanic eruptions, rocket launchings and high-altitude flights and also as a result of convective and synoptic processes in the atmosphere [5–9]. Frequently, dust grains strongly affect, and may even determine, environmental conditions.

Charged grains can lead to many physical effects having unique observable features [4, 5, 10–12]. The latter include ionospheric phenomena such as noctilucent clouds (NLC) and polar mesosphere summer echoes (PMSE), where dust grains result, in particular, from condensation of water vapor (see, *e.g.* [5]). The Earth's ionosphere can also become contaminated with dust particles as a result of bombardment by meteor showers. Ablation of the meteors at altitudes of 80 to 120 km in the lower ionosphere produces supersaturated vapors of metals, such as sodium, calcium, magnesium, *etc.* [13], which then condense into small grains with characteristic sizes of several nanometers to a few tenths of a micrometer. In the ionosphere, dust grains are charged due to photoelectric effect and the absorption of electrons and ions from the surrounding plasma. Therefore, the plasma of the dusty ionosphere can be considered as a dusty (complex) plasma [5]. Dusty plasma in the

https://doi.org/10.1017/S0022377809990675 Published online by Cambridge University Press

ionosphere can also be formed [14] during active geophysical rocket experiments, which, *e.g.* can use the scheme of the experiments 'Fluxus' and/or 'North Star' [15] and involve the release of some gaseous substance in near-Earth space. Dusty plasmas are present even in the lower atmosphere. For one thing, this concerns the plasma of lightning discharges containing nano- and microscale particles and can be important from the viewpoint of the properties of electromagnetic oscillations in the Schumann cavity [16]. The purpose of this paper is to review such plasma phenomena in the Earth's environments, where the processes inherent in dusty plasmas are important.

## 2. Radio noise from dusty ionosphere

Here we present the interpretation of the results of ground-based experiments carried out from 1999 to 2000 and in 2003 [17], measuring radio emission from the dusty ionosphere. These measurements allowed the authors to identify the characteristic features of the radio emission spectra typical for dusty ionospheric plasmas. The equipment and software specifically developed for this purpose make it possible to measure and study ionospheric radio noise with a registration characteristic time of 0.005 s. The equipment include, in particular, a modulation radiometer at $\lambda = 2$ m with a low-noise input amplifier (characterized by a noise temperature $T_{\rm noise} \sim$ 120 K) and an antenna (in the meter band) system with a mobile measuring complex.

Studies of the Fourier spectra of the ionospheric radio noise indicated that maxima ('dust' lines) are present in the spectra in addition to the known types of noise. It is thus possible to conclude that a dusty plasma component, which manifests itself in the frequency band of 12–50 Hz, exists in the ionosphere during the meteor showers. According to Musatenko et al. [17], this frequency band can be attributed to either the emission from the ionospheric layers, where the density of the charged particles is considerably enhanced during the meteoric showers, or to the modulation of the ionospheric emission. The distinguishing feature of the studies carried out in [17] is the use of an accurate and precise procedure for singling out disturbances of the radio noise spectra.

Several mechanisms that might be responsible for the origin of dust lines were proposed, in particular, they were interpreted as disturbances, as Schumann resonant harmonics, as the result of nonlinear non-dusty processes in the ionospheric F region or of nonlinear modulations in the entrance of the radiometer or of the scattering of radiation by turbulent pulsations in the troposphere or ionosphere [17]. Yet, none of them can explain why the lines were observed exactly during the high-speed meteor fluxes mentioned above.

The frequency range of 12–50 Hz is typical of a dust acoustic (DA) mode [18]. The generation of radio noise fluctuations can be attributed to the presence of dust grains condensed from supersaturated vapors of substances and materials that come into the ionosphere as a result of the ablation of meteors [19]. Note that, since DA waves are longitudinal, they exist only in a plasma and cannot reach the Earth's surface, where the measurement equipment [17] was installed. Therefore, only electromagnetic waves can be observed at the Earth's surface.

The low-frequency (LF) emission (12–50 Hz) corresponds to wavelengths of electromagnetic waves exceeding or of order of the Earth's radius. Such wavelengths could not be observed in the experiments [17]. Hence, the presence of the LF

https://doi.org/10.1017/S0022377809990675 Published online by Cambridge University Press

component in the electromagnetic wave spectrum is an indication of modulation of the electromagnetic waves escaping from the ionosphere. The wave modulation can result, *e.g.* from the modulational interaction [20] between the electromagnetic waves and DA waves. The dispersion relation of the DA waves in the ionospheric plasma at altitudes of 80 to 120 km is

$$\omega_s(k) = \sqrt{\frac{\omega_d^2}{b(k)} - \left(\frac{\nu_{dn}}{2}\right)^2} - i\frac{\nu_{dn}}{2}, \tag{2.1}$$

where $\omega_d^2 = 4\pi n_{d0} q_{d0}^2/m_d$ is the dust plasma frequency, $n_d$ is the number density of dust particles, $q_d$ is the dust particle charge, $m_d$ is the dust particle mass, $\nu_{dn} = (4/3)\,\pi a^2 \sqrt{8T_{n0}/\pi m_n}\, n_n\,(m_n/m_d)$ is the effective dust-neutral collision frequency, $n_n$, $m_n$ and $T_{n0}$ are the number density, the mass and the temperature of neutrals, respectively and $a$ is the dust particle size. The subscript 0 corresponds to unperturbed values. In the case of positive dust charges we obtain [19]

$$b(k) = 1 + \frac{1}{k^2\lambda_{De}^2}\left(1 + \frac{\bar{\nu}_e}{\nu_{ch}}\right), \tag{2.2}$$

and for $q_d < 0$ we have

$$b(k) = 1 + \frac{1}{k^2\lambda_{De}^2}\left(1 + \frac{1+\tau}{\tau}\frac{\bar{\nu}_e}{\nu_{ch}}\right) + \frac{1}{k^2\lambda_{Di}^2}, \tag{2.3}$$

where $\lambda_{De(i)} = \sqrt{T_{e(i)}/4\pi n_{e(i)} e^2}$ is the electron (ion) Debye length, $-e$ is the electron charge, $T_{e(i)}$, $n_{e(i)}$ and $m_{e(i)}$ are the electron (ion) temperature, number density and mass, respectively, $\tau = T_{i0}/T_{e0}$, $\bar{\nu}_e$ is the electron–dust collision frequency, $\nu_{ch} = -\left[\partial I^{eq}(q_d)/\partial q_d\right]_{q_d = q_{d0}}$ is the characteristic dust particle-charging frequency, $I^{eq}(q_d)$ is the total (including electron, ion and for $q_d > 0$ photoelectric) microscopic current on the dust particle [19].

During the Perseid, Orionid, Leonid and Geminid meteor showers, the LF background radio noise fluctuations can be substantially enhanced by the modulational interaction of the electromagnetic waves in the ionospheric plasma when dusts are present. It is suggested that the observed radio noise fluctuations (dust lines) stem directly from the modulational instability. Under this circumstance, the fluctuations are the LF virtual electrostatic fields (which are, in general, non-propagating fields) that are excited by the HF fields (here the electromagnetic waves) [20]. The peaks that appear against the background of LF virtual fields can be associated with DA waves, which obey a given dispersion relation [20], and can thus correspond to the spectral density peaks [17] characterizing the structure of the dust lines.

The main conclusions concerning the development of the modulational instability of electromagnetic waves in the lower dusty ionosphere are the following [19]. Perturbations on the ion acoustic time scales are suppressed there by ambipolar diffusion. Thus, the modulational instability gives rise to LF electromagnetic fields that can be associated with modulation by the DA mode. The modulational instability is caused by Joule heating, the ponderomotive force as well as the processes related to the charging of dust grains and their dynamics. For $q_{d0} < 0$ [21] (*e.g.* at night time when photoemission is absent), the modulationally excited LF (dust acoustic) perturbation frequency $\Omega$ and the maximum growth rate of the

https://doi.org/10.1017/S0022377809990675 Published online by Cambridge University Press

modulational instability $\Gamma$ are given by the expression [19]

$$\Omega \sim \Gamma \sim \left(\frac{\nu_e c^2}{\chi_e}\right)^{1/2} \frac{\omega_{pe}^6}{\nu_e \omega_0^5} \frac{|\mathbf{E}_0|^2}{4\pi n_{e0} T_{e0}}. \tag{2.4}$$

For $q_{d0} > 0$ [22] and $\Omega \gg \omega_{\chi e} \gg C_{Sd} K$, we have [19]

$$\Omega \sim \Gamma \sim \left[\nu_e \omega_{pe}^2 \left(\frac{\omega_{pe} C_{Sd}}{\omega_0 c}\right)^2\right]^{1/3} \left(\frac{|\mathbf{E}_0|^2}{4\pi n_{e0} T_{e0}}\right)^{1/3}, \tag{2.5}$$

and in the case $q_{d0} > 0$ and $\omega_{\chi e} \gg \Omega \gg C_{Sd} K$, the perturbation frequency and the growth rate are [19]

$$\Omega \sim \Gamma \sim \left(\omega_0 \frac{C_{Sd}^2}{\chi_e} \frac{\omega_{pe}^4}{\omega_0^4}\right)^{1/2} \left(\frac{|\mathbf{E}_0|^2}{4\pi n_{e0} T_{e0}}\right)^{1/2}. \tag{2.6}$$

Here, $\mathbf{E}_0$ and $\omega_0$ are the amplitude and the frequency of the electromagnetic pump wave repectively, $\omega_{\chi e} = \chi_e K^2$, $K = |\mathbf{K}|$ is the length of the wave vector of the modulational perturbations, $\chi_e = 3.16 T_e / m_e \nu_e$ is electron thermal conductivity coefficient, $\nu_e$ is the electron collision frequency, $\omega_{pe} = \sqrt{4\pi n_e e^2 / m_e}$ is the electron Langmuir frequency, $c$ is the speed of light and $C_{Sd} = |q_{d0}/e| \sqrt{n_d T_e / n_e m_d}$ is the dust acoustic speed.

Clearly, the modulational instability can develop only when its growth rate appreciably exceeds the damping rate $\nu_{dn}/2$ of the DA waves. For a wide range of ionospheric parameters, this damping rate is about $\nu_{dn} \sim 0.01 - 0.1\ \mathrm{s}^{-1}$. It is this value that determines the threshold for the modulational instability of electromagnetic waves in a plasma. This instability threshold agrees well with that deduced from observations, $\Omega > \nu_{dn}/2$ [19].

Thus, the mechanism for generating LF ionospheric noise [17] can be summarized as follows. During Perseid, Orionid, Leonid and Geminid meteor showers, the meteors are ablated at altitudes of 80–120 km, depending on their sizes and initial velocities. The result of the ablation is production of supersaturated vapors of metals, such as sodium, calcium, magnesium, *etc.*, which then condense into nanometer- to micrometer-sized secondary (dust) grains of cosmic origin. The grains can acquire electric charge because of unbalanced electron and ion currents to them and because of the photoemission resulting from solar radiation. As electromagnetic waves propagate in the dusty lower ionosphere, modulational interaction can excite LF electrostatic perturbations at characteristic frequencies close to that of the DA waves. As a result the electromagnetic waves become modulated. It is the LF component of the modulated wave against the ionospheric noise background that is recorded at the Earth's surface [17].

## 3. Other manifestations of DA waves

Here, we discuss other manifestations of DA perturbations excited by the modulational instability of electromagnetic waves in the ionosphere. The frequency of the DA waves lies in the infrasonic range, from several hundredths of a hertz to several tens of hertzs. This points to a possibility of excitation of infrasonic waves by the DA perturbations interacting with neutrals [19].

https://doi.org/10.1017/S0022377809990675 Published online by Cambridge University Press

The upper frequency of the infrasonic range is generally thought to be 16–25 Hz. The lower frequency of the range is uncertain. Infrasonic waves occur during earthquakes, underwater and underground explosions, storms and hurricanes, tsunamis, volcanic eruptions and so on. Among the main anthropogenic sources of infrasonic waves are chemical and nuclear explosions and also high-power enginery (in particular, rail and motor transport, aviation, rockets and great industry). Since infrasonic waves are weakly absorbed in air, as well as in water and within the Earth's crust, they propagate over very long distances and serve as indicators of cataclysmic events, such as storms, hurricanes, tsunamis *etc.*

For a fixed wavelength of the modulation, the maximum amplitude of the electrostatic potential $\varphi$ in the DA perturbation excited due to the modulational instability is

$$\varphi_0 \approx 8\pi q_{d0} \frac{n_{e0}}{K^3} \left(\frac{C_{Sd}}{c}\right)^2 \frac{\Omega}{\omega_0} \frac{|\mathbf{E}_0|^2}{4\pi n_{e0} T_{e0}}. \tag{3.1}$$

Dust-neutral collisions result in the appearance of forced or driven oscillations (at the same frequency and wave vector as that of the DA perturbation) of the neutrals. The forced neutral particle oscillation is a source for infrasonic waves. The evolution of the latter can be described by the wave equation with a forcing term on the right-hand side (see Sec. 75 of [23]),

$$\frac{1}{C_S^2} \frac{\partial^2 P_{n1}}{\partial t^2} - \Delta P_{n1} = \rho_0 \nabla \cdot (\mathbf{v}_n \cdot \nabla \mathbf{v}_n), \tag{3.2}$$

where $\mathbf{v}_n$ is the speed acquired by the neutrals due to their interaction with dust acoustic perturbations, $\rho_0$ and $C_S$ are the background mass density of neutrals and the acoustic speed at the corresponding altitude, respectively.

A typical vertical size of a dust layer in the lower dusty ionosphere is usually of the order of 1 km [24]. This value is much less than the characteristic size of the vertical atmospheric inhomogeneity. Thus (3.2) can be treated as a retarded potential equation and solved by standard methods [23].

The estimate of the maximum amplitude of infrasonic waves at the Earth's surface, obtained on the basis of (3.2), gives

$$P_{n1,\max} \sim \frac{\rho_0 V_1}{4\pi h_0} \frac{\delta K}{K} \left(\frac{\varphi_0 n_{d0} q_{d0}}{P_{n0}}\right)^2 \frac{\exp(m_n g h_0 / 2T_{n0})}{\Omega^{-2} + \nu_{dn}^{-2}}, \tag{3.3}$$

where $V_1$ is the volume of the dust cloud, $P_{n0}$ is the background pressure at the altitude $h_0$ of the dust cloud, $\delta\mathbf{K}$ is the characteristic wave vector of infrasonic wave (determined by the sum of two wave vectors of the dust acoustic perturbations) and $h_0$ is the altitude of dust layer localization.

For a wide range of dusty lower-ionosphere parameters [25], $T_n = 130$–$200$ K, $n_n = 10^{12}$–$10^{15}$ cm$^{-3}$, $a \sim 1$–$10^3$ nm, $n_d = 10$–$10^3$ cm$^{-3}$, $n_e \sim n_i \sim 10^4$–$10^5$ cm$^{-3}$, we find that the amplitude $P_{n1,\max}$ can reach the values of the order of 1 to 10 Pa. Fig. 1 displays the amplitude–frequency characteristics showing how infrasonic waves from various sources (in particular, large and small explosions, Rayleigh waves during earthquakes, magnetic substorms, hurricanes, tornadoes, supersonic aircraft, microbaroms and thunderstorms, mountain wave activity and so on) are distributed near the Earth's surface. Curve 7 characterizes infrasonic waves originating from DA waves in the Earth's lower ionosphere during meteor showers. The dependence (7) has been determined using the following parameters:

https://doi.org/10.1017/S0022377809990675 Published online by Cambridge University Press

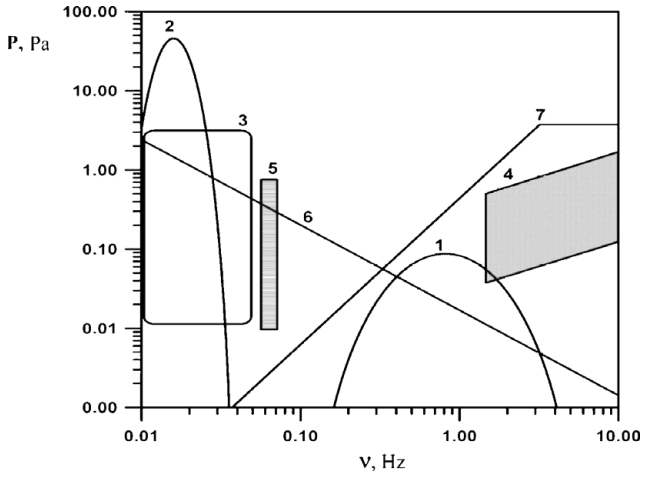



**Figure 1.** Amplitude–frequency characteristics showing how infrasonic waves from various sources are distributed near the Earth's surface: (a) the region of infrasonic perturbations originating from small explosions; (b) the region of infrasonic perturbations originating from large explosions; (c) the region of infrasonic waves from Rayleigh waves during earthquakes, magnetic substorms, hurricanes, tornadoes and mountain wave activity; (d) the region of infrasonic waves generated by supersonic aircraft and thunderstorms; (e) the region of infrasonic waves from microbaroms; (f) the local turbulent noise region and (g) the region of infrasonic waves excited by a DA mode during meteor fluxes.

$h_0 \approx 90$ km, dust cloud typical vertical size is of the order of 1 km, the characteristic size of dust grains is $a \approx 25$ nm, $n_d \approx 10^2$ cm$^{-3}$, $n_e \approx 10^5$ cm$^{-3}$ and $T_n = 140$ K. It is seen that for frequency band from a few tenths of Hz to several dozens of Hz of the dust acoustic perturbations, their excitation during Perseids, Orionids, Leonids and Geminids meteor showers is the most important source of infrasonic waves at the Earth's surface.

Dust acoustic perturbations can also serve as a source of acoustic gravitational waves (AGWs), which have wavelengths greater than or of the order of 1 km and frequencies in the infrasonic range. Here we consider the main effects [19] by which AGWs show up during meteor fluxes and can be observed from the Earth's surface.

The AGWs are convectively unstable at altitudes of 110–120 km. Due to the instability, these waves can grow in amplitude. Moreover, the only growing waves are those that pass through the convective instability zone. When the amplitudes of the AGWs generated by DA perturbations during meteor fluxes grow to values of the order of the background pressure of the surrounding medium, the linear wave process becomes nonlinear. The competition between the nonlinear effects and the effects of dispersive spreading can give rise to steady localized nonlinear vortex structures [26]. Note that at altitudes of 110–120 km, the dust density is low, so the dust acoustic perturbations generated there by the modulational instability are unlikely to grow at a rate much faster than the growth rate of the AGWs, $\gamma_a \approx 0.2$ s$^{-1}$. In analogy with conventional acoustic waves, the generation of AGWs by dust acoustic perturbations is a far slower process than the development of the modulational instability. Consequently, whereas the amplitude of the conventional acoustic wave is determined by the amplitude of the DA perturbation, the convective instability at altitudes of 110–120 km causes an AGW to evolve in a

https://doi.org/10.1017/S0022377809990675 Published online by Cambridge University Press

different way, specifically, the most important processes governing the amplitude of acoustic gravitational perturbations are nonlinear processes that give rise to acoustic gravitational vortices, while the modulational instability serves merely to trigger acoustic gravitational perturbations.

The vortex structures can increase the intensity of green nightglow. At altitudes of 80–120 km, the green line is excited by the two-step Barth–Hildebrandt mechanism, consisting of the following two reactions:

$$\mathrm{O}(^3\mathrm{P}) + \mathrm{O}(^3\mathrm{P}) + \mathrm{M} \rightarrow \mathrm{O}_2^* + \mathrm{M}, \tag{3.4}$$

$$\mathrm{O}_2^* + \mathrm{O}(^3\mathrm{P}) \rightarrow \mathrm{O}_2 + \mathrm{O}(^1\mathrm{S}), \tag{3.5}$$

with subsequent emission of the green line ($\lambda = 557.7$ nm) in the reaction

$$\mathrm{O}(^1\mathrm{S}) \rightarrow \mathrm{O}(^1\mathrm{D}) + 2\pi\hbar/\lambda. \tag{3.6}$$

Here $\mathrm{O}(^3\mathrm{P})$ is atomic oxygen in its ground state, $\mathrm{O}_2^*$ is molecular oxygen in excited state, M is an arbitrary neutral molecule and $\mathrm{O}(^1\mathrm{S})$ and $\mathrm{O}(^1\mathrm{D})$ are the forms of atomic oxygen in excited state.

The intensity of the emitted green line is proportional to the third power of the atomic oxygen density [26]. The density of atomic oxygen can vary because of the presence of localized nonlinear vortex structures or dust Rayleigh–Taylor instabilities [26]. The appearance of such dust-driven vortices and instabilities can result in a convective overturn of oxygen in vertical direction and thus in an enhancement of the atomic oxygen density at 110–120 km. For the characteristic conditions of the normal atmosphere at altitudes of about 110 km we obtain

$$\frac{\Delta I}{I_s} \sim \left(1 + 10^{-2}u\right)^3 - 1, \tag{3.7}$$

where $I_s$ is the mean seasonal green emission intensity and $\Delta I = I_{Ob} - I_s$, with $I_{Ob}$ being the observed green line intensity and $u$ the speed of the steady waves propagating horizontally. For the characteristic velocities $u$ ($u \leqslant 130$ ms$^{-1}$), the ratio $\Delta I/I_s$ can be about 10%, a level detectable on the Earth's surface [27].

Thus, excitation of infrasonic waves by the modulationally excited DA perturbations can result in two observational manifestations: (a) direct observation of infrasonic acoustic waves at the Earth's surface, and (b) amplification of the intensity of the green emission at 557.7 nm from the region of the lower ionosphere at the altitudes of 110 to 120 km.

## 4. Polar mesospheric dust clouds

One important feature of the polar mesosphere under summer conditions is the presence of dust layers (very thin on the atmospheric scale) located at altitudes of 80 to 85 km (NLC) or 85 to 95 km (PMSE). NLC consist of submicron-sized particles. Their vertical optical thicknesses are much less than unity, but they can be seen by the naked eye at sunset, whereas PMSE (apparently consisting of charged nanoscale particles) cannot be observed by optical methods and manifest themselves by strong radio reflections observed with radars at frequencies between 50 MHz and 1000 MHz [28]. Strong correlation between observations of NLC and PMSE suggests that they have a common origin. In the literature, NLC and PMSE are frequently grouped together under the common term polar mesospheric clouds (PMC) [10].

https://doi.org/10.1017/S0022377809990675 Published online by Cambridge University Press

The formation of NLC and PMSE takes place in the polar atmosphere at mesospheric altitudes (80 to 95 km) between the end of May and the end of August. In this period, the ambient air temperature in the polar mesosphere falls below 150 K [10], and water vapor supersaturates. This leads to conditions favoring the growth of dust grains. The dominant nucleation mechanism appears to be the condensation of water molecules on nanoscale grains, which are always present at mesospheric altitudes. The characteristic grain size is a few nanometers [5, 25], and its density typically is 10 to 1000 $cm^{-3}$. Particle nucleation conditions are satisfied at altitudes between 78 km and 92 km, where water vapor is supersaturated. Note that it is in this altitude range where NLC and PMSE are observed.

Microscopic currents of electrons and ions in the ambient plasma and their recombination on the surface of a dust particle result in its charging. This leads to a considerable decrease in positive-ion and electron densities in the regions occupied by NLC and PMSE. Effects due to solar radiation may lead to much more complicated behavior of charged species in dusty ionospheric plasmas, depending on the photoelectric properties of dust particles, their density and grain size. A systematic analysis of sounding rocket flight experimental results concerning the behavior of charged species in the polar mesosphere under summer conditions shows that the following five trends can be identified [5]:

(a) Considerable dips ('bite-outs') in both electron and positive-ion densities at altitudes between 80 km and 85 km.

(b) Considerable decrease in the electron density without any significant change in the density or composition of the positive-ion subsystem.

(c) A considerable increase in electron density in the region occupied by NLC, while no measurements of ion densities were performed.

(d) A considerable increase in the density of positive ions accompanied by a dip in electron density.

(e) No appreciable change in the electron and positive-ion densities while strong radio reflections were observed in the mesosphere (at altitudes between 80 km and 85 km) in radar frequency bands of 50 to 1000 MHz. These results can be explained by the presence of dust particles in the middle atmosphere. For this purpose a theoretical model [5] has been developed, which provides a self-consistent description of spatiotemporal variations of the plasma composition in the polar mesosphere under summer conditions and formation of NLC and PMSE and takes into account sedimentation of dust grains in the middle atmosphere, their growth in a supersaturated water vapor and dust particle charging processes, allowing for variations of the ion subsystem composition in the polar mesosphere and photoelectric emission. Microscopic electron and ion currents incident on the grains are calculated by using the orbit-limited probe model (see, *e.g.* [5]), in which the cross sections for collisions of electrons and ions with a charged grain are determined by angular momentum and energy conservation laws.

Discuss the results obtained by applying the above theoretical model to the polar ionosphere at 80 to 95 km under summer conditions. Our discussion is focused [5] on the possibility of explaining the most important experimental data concerning behavior of charged species in a dusty ionosphere. The presence of submicron-sized particles in the mesosphere has a strong effect on plasma characteristics (depending on photoelectric properties of dust grain material). This effect is illustrated in Fig. 2 by spatiotemporal variations of mesospheric ion and electron densities in the presence of a layer of dust grains characterized by different values of the work function.

https://doi.org/10.1017/S0022377809990675 Published online by Cambridge University Press

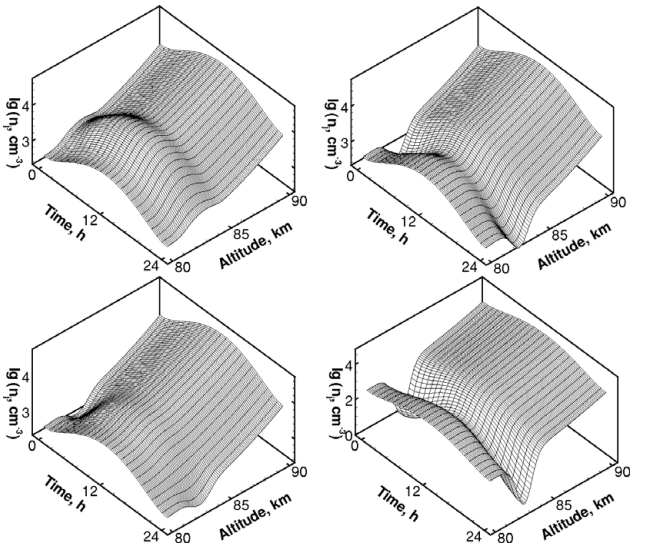



**Figure 2.** Effect of the photoelectric properties of a dust layer on the electron and ion densities in the lower ionosphere. The right panels correspond to the absence of photoelectric emission from dust grains (the work function exceeds 7.3 eV, the cutoff of the solar spectrum at the mesospheric altitudes [11], as in the case of pure ice dust particles). The left panels illustrate strong effect of photoelectric emission on the plasma composition in the mesosphere (work function below 7.3 eV, as in the case of calcium dust particles). Top and bottom panels are electron and ion densities.

The right panels correspond to pure ice dust particles. In this case, since there is no photoelectric emission, the dust particles are negatively charged and both ion and electron densities are reduced in the region occupied by the dust layer. It can be shown that a density $n_d \approx 10^2$ cm$^{-3}$ of dust grains of diameter $2a \approx 100$ nm is sufficient to substantially reduce the mesospheric plasma density. These dust grain parameters are common for NLC-type structures. It should be noted that a decrease in electron density reduces the loss of ions due to recombination. Therefore, while the presence of dust particles reduces the electron density, the ion density in the mesosphere may remain unchanged or even increase. These effects obviously depend on the relative importance of the ion losses due to recombination and collisions with dust grains. As the dust grain density exceeds a certain value, the equilibrium ion density becomes independent of the electron density and is controlled only by the loss of ions in collisions with dust particles, because the electron density is substantially reduced and the role played by ion losses due to recombination is insignificant. The left panels in Fig. 2 correspond to a dust particle material characterized by a relatively low work function ($W \approx 3$ to 4 eV). In this case, even if the dust particle density is low ($n_d \sim 10$–$100$ cm$^{-3}$), the model [5] predicts an increase in electron density and a decrease in ion density, due to higher recombination losses.

Note that the mesospheric plasma exhibits a more diverse behavior when photoelectric emission plays a significant role. Depending on the dust particle size and density, virtually any effect due to the presence of dust particles in the mesosphere can be observed. Thus the model [5] can be used to predict the five trends (a)–(e) associated with NLC and PMSE as enumerated above. The model [5] provides a

https://doi.org/10.1017/S0022377809990675 Published online by Cambridge University Press

unified explanation of these trends and of the presence of both positively and negatively charged particles in the upper atmosphere discovered by means of sounding rocket flights, as well as of the experimental fact that neither NLC nor PMSE can be observed permanently.

## 5. Some other examples

Applications of methods developed in studies of dusty plasma are also important for adequate description of such problems of Earth's sciences as active geophysical rocket experiments, formation of terrestrial planets, Schumann resonances *etc*. Here we outline the role of dusty plasma effects in these problems.

### 5.1. Active rocket experiments

The problem of interest is to investigate the possibility of an appearance of charged dust particles in active rocket experiments, which involve the release of some gaseous substance in near-Earth space. This can be reached using the scheme of the experiments analogous to that of the 'Fluxus' and 'North Star' experiments carried out in the ionosphere at altitudes of 140, 280 and 360 km [15]. The source for the charged particle release in the ionosphere in these experiments is the generator of high-speed plasma jets. Dust particles in the experiments appear as a result of condensation. The period of the formation of the centers of condensation is very short, and all drops have approximately the same size [14, 29]. The formation of the dust particles in the active rocket experiments is confirmed by the results of both active and (modeling them) laboratory experiments, as well as numerical simulations. In the first injection of the 'North Star' experiment positively charged clusters of aluminium consisting of 2, 4, 8 and 16 atoms were detected in the jet. The clusters of larger masses could not be detected because of the narrow range of the measured cluster energies. However, the analysis of electromagnetic radiation from the jet in the infra-red range of the spectrum shows the presence of micrometer-sized charged drops.

In [14] the idea of the formation of shocks related to dust charging in the active rocket experiments has been forwarded, which involve the release of some gaseous substance in near-Earth space. The shock wave front is associated with the fore (border)-part of the jet propagating in the plasma of the ionosphere. Drops appearing as a result of condensation are charged due to their interaction with the ambient plasma and the photoelectric effect. The optimum speeds of the jet are 10 $\mathrm{kms}^{-1}$. The optimum altitudes for such experiments are 500–600 km.

The active experiments, where the shocks in charge-varying dusty plasmas are observed, can be helpful to model different physical phenomena occurring in nature, *e.g.* in the process of a large meteoroid impact with the Moon surface [30]. The evolution of the impact plume can lead to the formation of shock wave structure associated with an appearance of charged microparticles, which are created in the process of condensation of the substance of vapor plume and thrown from the crater and surrounding its regolith layer.

### 5.2. Primary earth

The theory and data of comparative planetology as well as the Earth sciences (consistent with each other) enable us to state that the formation of the terrestrial planets occurred during 30–100 million years beginning from an appearance of

https://doi.org/10.1017/S0022377809990675 Published online by Cambridge University Press

the first condensate approximately $4.6 \times 10^9$ years ago [31]. During the Earth's growth the main energy source was related to impacts of cosmic bodies falling to the growing planet. The mass spectrum of the cosmic bodies is considered to be proportional to $m^{-q}$, where $q \approx 1.8 \pm 0.2$. The main mass is concentrated in the bodies with diameters of 100 km and larger. Craters formed as a result of the impact of such large bodies with the Earth's surface are estimated to have depths of the order of the Earth's diameter. The matter of the impact-generated vapor plume has the mass of the order of the cosmic body (impacting the Earth), while its temperature reaches several electron-volts. All this matter expands (lifts) with subsequent ionization, cooling, condensation and formation of nano- and microscale dust particles and their charging. Thus, the dusty plasma is formed. The important problem is to determine the characteristic sizes of the dust particles and estimate their mass spectrum because these will allow us to determine behavior of the dust grains: whether they work to the primary Earth's surface or evolve in the primary atmosphere. This study will allow us to update the scenario of the formation of the primary Earth's crust, hydrosphere and atmosphere and possibly to modify the scenario of the origin of terrestrial planets.

### *5.3. Schumann resonances (SRs)*

Schumann resonances represent global electromagnetic oscillations excited by lightning discharges in a concentric spherical cavity formed by the Earth's surface and the lower ionosphere. As a rule, four or five first resonance peaks are recorded. The peak frequencies vary within several tenths of a hertz near frequencies of about 8, 14, 20 and 26 Hz. The presence of dust grains in the Earth–ionosphere cavity can significantly enhance thunderstorm activity. Since this activity is directly related to the SR amplitude, an increase in the concentration of nano- and microscale particles in the atmosphere can raise the efficiency of energy pumping of the cavity [16]. For example, during violent volcanic eruptions, the SR amplitude can increase several-fold. The presence of dust particles in the atmosphere also influences the annual average temperature near the Earth's surface. For instance, violent volcanic eruptions are accompanied by an appreciable decrease in the annual average temperature. Since the SR amplitude is related to the surface temperature, a decrease in the temperature can lead to a decrease in the energy density in the cavity. Furthermore [16], the presence of dust particles in the lower ionosphere affects its dispersion properties, decreasing the frequencies and quality of the resonances.

## 6. Summary

Thus, we have described possible observational manifestations of dusty ionospheric plasmas during high-speed meteor showers, namely, ground-based observations of low-frequency ionospheric radio noise with the frequencies lower than 50 Hz, ground-based observations of infrasonic waves and amplification of the intensity of green emission at the wavelength of 557.7 nm from a layer of lower ionosphere located at 110–120 km. We have discussed physical processes accompanying the formation of NLC and PMSE and presented a unified explanation of ionization properties of the polar mesosphere under summer conditions. Furthermore, we have considered dusty plasma processes in application to the description of active geophysical rocket experiments, which involve release of some gaseous substance

https://doi.org/10.1017/S0022377809990675 Published online by Cambridge University Press

in the near-Earth space, the origin of the primary Earth's crust, hydrosphere and atmosphere, and the global electromagnetic Schumann resonances.

*Acknowledgements*

This study was supported by the Division of Earth Sciences, Russian Academy of Sciences (the basic research program 'Nanoscale particles in nature and technogenic products: conditions of existence, physical and chemical properties, and mechanisms of formation') and the Division of Physical Sciences, the Russian Academy of Sciences (the basic research program 'Plasma physics in the solar system'). The author is also supported by the Dynasty Foundation.

## References

[1] Fortov, V. E., Ivlev, A. V., Khrapak, S. A., Khrapak, A. G. and Morfill, G. E. 2005 *Phys. Rep.* **421**, 1–103.

[2] Ostrikov, K. 2005 *Rev. Mod. Phys.* **77**, 489–511.

[3] Vladimirov, S. V., Ostrikov, K. and Samarian, A. A. 2005 *Physics and Applications of Complex Plasmas*. London: Imperial College Press.

[4] Verheest, F. 1994 *Space Sci. Rev.* **68**, 109–114.

[5] Klumov, B. A., Morfill, G. E. and Popel, S. I. 2005 *JETP* **100**, 152–164.

[6] Popel, S. I. and Gisko, A. A. 2006 *Nonlinear Proc. Geophys.* **13**, 223–229.

[7] Holton, J. R., Haynes, P. H., McIntyre, M. E., Douglass, A. R., Rood, R. B. and Pfister, L. 1995 *Rev. Geophys.* **33**, 403–439.

[8] Fromm, M. D. and Servranckx, R. 2003 *Geophys. Res. Lett.* **30**, 1542, doi: 10.1029/2002GL016820.

[9] Besedina, Yu. N. and Popel, S. I. 2008 *Doklady Earth Sciences* **423A**, 1475–1478.

[10] Gadsen, M. and Schröder, W. 1989 *Noctilucent Clouds*. Berlin: Springer.

[11] Klumov, B. A., Popel, S. I. and Bingham, R. 2000 *JETP Lett.* **72**, 364–368.

[12] Kopnin, S. I., Kosarev, I. N., Popel, S. I. and Yu, M. Y. 2004 *Planet. Space Sci.* **52**, 1187–1194.

[13] McNeil, W., Lai, S. and Murad, E. 1998 *J. Geophys. Res.* **103**, 10 899–10 911.

[14] Popel, S. I. and Tsytovich, V. N. 1999 *Astrophys. Space Sci.* **264**, 219–226.

[15] Gavrilov, B. G., Podgorny, A. I., Podgorny, I. M., Sobyanin, D. B., Zetzer, J. I., Erlandson, R. E., Meng C.-I. and Stoyanov, B. J. 1999 *Geophys. Res. Letters* **26**, 1549–1552.

[16] Besedina, Y. N. and Popel, S. I. 2007 *Plasma Phys. Reports* **33**, 138–145.

[17] Musatenko, S. I., Musatenko, Y. S., Kurochka, E. V., Lastochkin, A. V., Cholij, V. Y., Maksimenko, O. I. and Slipchenko, A. S. 2006 *Geomagn. Aeronomy* **46**, 173–182.

[18] Rao, N. N., Shukla, P. K. and Yu, M. Y. 1990 *Planet. Space Sci.* **38**, 543–546.

[19] Kopnin, S. I., Popel, S. I. and Yu, M. Y. 2009 *Phys. Plasmas* **16**, 063705.

[20] Popel, S. I., Vladimirov, S. V. and Tsytovich, V. N. 1995 *Phys. Rep.* **259**, 327–405.

[21] Shukla, P. K. and Vladimirov, S. V. 1995 *Phys. Plasmas* **2**, 3179–3183.

[22] Shukla, P. K. and Stenflo, L. 2001 *IEEE Trans. Plasma Sci.* **29**, 267–270.

[23] Landau, L. D. and Lifshitz, E. M. 1987 *Fluid Mechanics*. Oxford: Pergamon.

[24] Hunten, D. M., Turco, R. P. and Toon, O. B. 1980 *J. Atmos. Sci.* **37**, 1342–1357.

[25] Havnes, O., Aslaksen, T. and Brattli, A. 2001 *Phys. Scripta* **T89**, 133–137.

[26] Aburdzhaniya, G. D. 2006 *Self-Organization of Vortex Structures and Vortex Turbulence in Dispersive Media* [in Russian]. Moscow: KomKniga.

[27] Brasseur, G. and Solomon, S. 1984 *Aeronomy of the Middle Atmosphere*. Dordrecht, Netherland: Reidel.

https://doi.org/10.1017/S0022377809990675 Published online by Cambridge University Press

[28] Cho, J. Y. N. and Röttger, J. 1997 *J. Geophys. Res.* **102**, 2001–2020.

[29] Popel, S. I., Gisko, A. A., Golub', A. P., Losseva, T. V., Bingham, R. and Shukla, P. K. 2000 *Phys. Plasmas* **7**, 2410–2416.

[30] Nemtchinov, I. V., Shuvalov, V. V., Artemieva, N. A., Kosarev, I. B. and Popel, S. I. 2002 *Intern. J. Impact Engineering* **27**, 521–534.

[31] Vitjazev, A. V., Pechernikova, G. V. and Safronov, V. S. 1990 *Terrestrial Planets: Origin and Early Evolution*[in Russian]. Moscow: Nauka.

https://doi.org/10.1017/S0022377809990675 Published online by Cambridge University Press